Paleobiology, 40(3), 2014, pp. 494–509
DOI: 10.1666/13051

Growth oscillation in larger foraminifera

Antonino Briguglio and Johann Hohenegger

Abstract.—This work shows the potential for applying three-dimensional biometry to studying cell growth in larger benthic foraminifera. The volume of each test chamber was measured from the three-dimensional model obtained by means of computed tomography. Analyses of cell growth based on the sequence of chamber volumes revealed constant and significant oscillations for all investigated specimens, characterized by periods of approximately 15, 30, 90, and 360 days. Possible explanations for these periods are connected to tides, lunar cycles, and seasonality. The potential to record environmental oscillations or fluctuations during the lifetime of larger foraminifera is pivotal for reconstructing short-term paleoenvironmental variations or for gaining insight into the influence of tides or tidal current on the shallow-water benthic fauna in both recent and fossil environments.

Antonino Briguglio and Johann Hohenegger. Department of Palaeontology, University of Vienna, Vienna 1090, Austria. E-mail: antonino.briguglio@univie.ac.at.* *Present address*: Naturhistorisches Museum Wien, Vienna 1010, Austria*

Accepted: 27 January 2014
Published online: 7 May 2014

Introduction

Larger benthic foraminifera (LBF) are large-sized shallow-water marine protists that host symbiotic microalgae, and whose tests (shells) have to function as glass houses to let light penetrate them (Hottinger 1982). Because of their high evolutionary rates, great diversity, and exceptional abundance in fossil and Recent oligotrophic tropic and warm temperate marine environments, LBF are routinely used in biostratigraphy (e.g., Serra-Kiel et al. 1998; Egger et al. 2013) and paleoenvironmental analyses (e.g., Beavington-Penney and Racey 2004, Gebhardt et al. 2013).

Large cell volumes, giving space for symbiotic microalgae, enable independence from food capture to various degrees; therefore LBF are mixotrophic organisms approximating autotrophs in some genera (Hallock 1985). In deeper regions of the photic zone the need to increase the number of photosymbionts is satisfied by flat and thin tests, which raise the test surface-to-volume ratio in response to decreasing light intensity (Hohenegger 2009). Thin and flat tests (i.e., high surface-to-volume ratio) are also well adapted to low hydrodynamics, typical of deeper environments; in higher-energy environments, in contrast, LBF build thicker and rounded tests with higher settling velocity to avoid transport (Hohenegger 2009). Shape and size of these tests are thus in perfect equilibrium with the surrounding environment (Hottinger 2000; Briguglio and Hohenegger 2011).

Because the foraminiferal shells are compartmentalized into chambers, and sometimes into chamberlets, the cell has to maintain its environmental equilibrium during all growth stages (Schmidt et al. 2013). Therefore, the shape and size of each single chamber provides highly temporally resolved information on the environment (Briguglio and Hohenegger 2009; Briguglio et al. 2013) and on cell ontogeny, which is represented by the sequence of chambers (Hottinger 2000; Briguglio et al. 2011). Such information is provided by the genetic system of the foraminiferal cell, which controls the growth and all its stages (Tyszka 2004).

The functional morphology of LBF tests has been investigated from many perspectives; however, such studies have been hampered by their two-dimensional approach to observation and measurement of the shells: by means of either thin section or polished specimens. Thus, all results achieved so far are mainly based on simple parameters such as diameters, angles, and distances. We therefore used high-resolution computed tomography (CT) because it is possibly the best method to get

 0094-8373/14/4003-00/$1.00

quantitative data on three-dimensional objects, such as size and volume of the chambers of foraminifera.

The use of CT in natural sciences and particularly in paleontology has become quite common for investigation of surfaces or internal structures in a hollow object. The potential of this technique for studying foraminifer has been already described (Speijer et al. 2008), and the first results concerning visualizations and basic measurements are gradually appearing in journal articles (Briguglio and Benedetti 2012; Hohenegger and Briguglio 2012; Görög et al. 2012); new species have even been described following CT biometric investigation (Benedetti and Briguglio 2012), with available type material being used as online three-dimensional models. Here we explore volumetric measurements of three-dimensional objects (i.e., chamber volume) as a tool for estimating growth patterns and oscillations.

Growth in biology—either in organisms or in populations and clones—can generally be fitted by mathematical models. The most commonly used functions are the exponential and the logistic growth models (Batschelet 1971). In LBF, cell growth represented by the test volume can best be fitted by the Gompertz function (see explanation below).

Oscillations around growth functions in individuals have been observed among various groups of organisms; the best examples are plants, but, among metazoans, oscillations were first recognized in fishes (Fulton 1901). Such growth oscillations are commonly related to seasonality expressed by temperature, salinity changes (in the case of marine organisms), or other environmental parameters. It is therefore not surprising that growth cycles are also evident in foraminifera, but their relations to orbital cycles of calendar band frequencies or to environmental factors are still unknown.

So far, most studies involving temperature variations and seasonality have been carried out on planktic rather than benthic foraminifera. Relative abundances, diversity, Mg/Ca ratios and stable isotopes are just the most common parameters measured on the test to gain insight into the environmental influences on foraminifers (Barker et al. 2005). Because the lifetime of planktic foraminifera is normally no more than several weeks, studying their growth response to environmental variation is virtually impossible. The only experiments run so far are based on multiple measurements of numerous specimens collected over time or along sedimentary sections, leading to the extrapolation of information such as changes in sea-surface temperatures and seasonal variations (Fraile et al. 2009) and latitudinal gradients (King and Howard 2005). LBF, however, live longer than planktic or smaller benthic foraminifera and may be most suitable for detecting growth variation and/or oscillation due to calendar band frequencies during their lifetime (Evans at al. 2013). Variations in cell growth have been already observed in both recent and fossil LBF (Briguglio et al. 2011, 2013) but they have not been studied in relation to time or related to environmental factors to estimate periodic oscillations.

This paper therefore focuses on growth oscillation of LBF and tries to test periodic environmental variations as causes of such oscillatory growth.

Materials and Methods

The available material for this study was collected in sandy substrates at 50 m depth at Belau (commonly known as Palau) in 1994 and at Sesoko Island, Japan, in 1996 (Fig. 1). Location, chamber number, and generation of the investigated specimens *Palaeonummulites venosus* (Fichtel and Moll) and *Cycloclypeus carpenteri* Brady are reported in Table 1. Further information on the sampling method and environment can be found in Hohenegger et al. (1999). For this study, all investigated specimens have been treated separately and only the relative sizes of their empty chambers contributed to the presented data set.

In many benthic foraminifera three generations can be found expressed in a trimorphic cycle (e.g., Röttger 1990; Dettmering et al. 1998). The haploid gamonts (megalospheres, A1 generation) are followed through sexual reproduction by diploid agamonts (microspheres, B generation) (sensu Hottinger

FIGURE 1. Study areas in the West Pacific. 1. Sesoko-Jima (for location details see Hohenegger et al. 1999); 2. Ishigaki-Jima (for location details see Kosuge et al. 1997); 3. Belau (for location details see Hohenegger 1996). Equator (Eq) and Tropic of Cancer (ToC) are indicated as dotted lines.

2006). Reproduction of agamonts leads to diploid schizonts (megalospheres, A2 generation) by mitosis or to haploid gamonts by meiosis. Schizonts can reproduce either by mitosis leading to schizonts again or by meiosis leading to gamonts. This trimorphic cycle is typical for LBF, where sexual reproduction by gametes becomes difficult in high-energy environments. The two megalospheric (A-) generations do not differ in shape except possibly for slight differences in proloculus size, which makes the distinction between gamonts and schizonts based solely on test form and size impossible. We have therefore combined gamonts and schizonts in our investigation.

We investigated each specimen by means of computed tomography with a high-energy Skyscan1173 at the Department of Palaeontology, University of Vienna, Austria (the specimen V0 was scanned at the Department of Theoretical Biology of the same university). Samples were scanned in small cylindrical plastic containers (a polypropylene pipette tip). Most plastics are relatively transparent to X-rays and thus are suitable for scanning mineralized specimens. The specimens were scanned in vertical position to reduce the thickness crossed by X-ray radiation, thus yielding more contrast. Cardboard was used to maintain them in position during rotation.

After reconstruction and equatorial re-slicing (sensu Briguglio et al. 2014), of all three-dimensional models, each chamber of the investigated specimens was extracted either manually or with a semiautomatic grayscale-based algorithm, and its volume was measured. Connections between successive chambers (or chamberlets for *Cycloclypeus carpenteri*) such as foramina or stolons were cut through their central part.

A large proportion of the investigated specimens of *C. carpenteri* revealed internal broken chambers that had always been repaired by the subsequent set of chamberlets. Because calculation of the volume of broken chambers might bias the data, specimens whose broken chambers constituted less than 15% of the total number of chambers were completely segmented, but the broken chambers were not included in the cumulative sum of chamber volumes.

After chamber extraction, linearization of chamber volumes was done by calculating their cubic roots. Linearization is mandatory when linear statistical methods have to be used on non linear variables like volumes.

In LBF, cell growth represented by the test volume V can best be fitted by the Gompertz function

$$V = K\exp\Big(b\exp(ct)\Big). \qquad (1)$$

It approximates an upper asymptote K comparable to the logistic function, and parameters b and c represent time displacement and growth rate (Hohenegger and Briguglio 2014).

When the first derivative of this function,

$$V' = \frac{dV}{dt} = -cV\ln\ (K/V), \qquad (2)$$

reaches the maximum ($V'' = 0$), this inflection point characterizes the change from increasing chamber volumes to decreasing ones during further growth. Therefore, the inflection point

marks the latest time of reproduction. In a few cases, however, reproduction is postponed by continuing cell growth, and this is expressed in chambers decreasing in size. Tests displaying this were first described in planktic foraminifera and called "kummerformen" (Olsson 1973).

The parameters K, b, and c of the Gompertz function (eq. 1) were calculated from the cumulative sum of linearized chamber volumes replacing time t by chamber number i (Hohenegger and Briguglio 2014). From this function, the expected chamber volumes could be calculated by using the first derivative of the Gompertz function (eq. 2). Afterwards, standardized residuals from the observed and the expected chamber volumes were calculated for each growth step.

The need for standardization is demonstrated by residuals increasing significantly with chamber number in both test and chamber volumes (Briguglio et al. 2011; Hohenegger and Briguglio 2014). Therefore, deviations from the non-linear Gompertz function are much smaller at early growth stages than at later growth stages. Standardized residuals are obtained by

$$d_i = \frac{(v_{oi} - v_{ei})}{v_{ei}}, \tag{3}$$

where d_i represents the residual, v_{oi} the observed, and v_{ei} the expected volume of the i^{th} chamber.

Standardized residuals were then analyzed for oscillations and cyclicity. This was done by plotting residuals against time, as represented by the chamber-building rate.

The chamber-building rate and lifetime of LBF are not yet fully known, but some studies provide insight into how fast such protists might grow. All published data refer to chamber-building rate measured under laboratory conditions, which are not easy to interpret for environmental analyses (Hohenegger et al. 2014). To estimate the chamber-building rate of *Cycloclypeus carpenteri*, we used the data collected by Lietz (1996). She cultivated and successfully let reproduce three (out of 20) agamonts collected at Sesoko-Jima (60-m depth) under laboratory conditions. After these reproductions she observed the growth rate of ~100 (out of 2000) young gamonts/schizonts from the first agamont and 40 (out of 400) from the second agamont. The gamonts/schizonts obtained from reproduction of the third agamont were studied by Krüger (1994), who also conducted laboratory experiments on *Palaeonummulites venosus*. The results reported in these two theses are represented either by diameter or by chamber number versus lifetime.

Concerning *C. carpenteri*, during the first weeks the observed growth rate was almost three chambers per week; it reduces to two chambers per week until the 17th week, and it drops again down to one chamber per week until the 24th week. Less than one chamber per week was produced on average until the 46th week. Such laboratory cultures gave specimens with an average chamber number of 67. Concerning *P. venosus*, the data provided by Krüger (1994) are very poor. A growth rate of one chamber per day was observed during the first week, at the end of the second week all individuals had 10 or 11 chambers, and from the fourth month the growth rate decreased to one chamber per week only.

The most accurate data set on growth rate and growth pattern on LBF was produced by observations on *Heterostegina depressa*. The main results were published by Röttger (1972) and Röttger and Spindler (1976).

The growth rate we propose here is based on a combination of all the information on *H. depressa* (Rötter 1972), *C. carpenteri* (Lietz 1996), and *P. venosus* (Krüger 1994). These data suggest that the best-suited function for expressing the growth rate is the power function, which has been estimated as

$$i = 2.849t^{0.509} \tag{4}$$

for *P. venosus* gamonts and schizonts and

$$i = 1.289t^{0.698} \tag{5}$$

for *C. carpenteri* gamonts, where t represents the day when chamber i was constructed (Fig. 2).

To obtain averaged timing for the construction of the i^{th} chamber, we used the inverse

TABLE 1. List of all specimens used in this study. The column "Ch." indicates the number of extracted chambers. See text for further information.

Specimen code	Taxon	A/B	Origin	Ch.	Gompertz parameter			Cycles			
V0	*P. venosus*	A	Sesoko	44	$K = 19.677$	$r^2 = 0.997$		$a = 0.093$	$a = 0.0822$	$a = 0.0758$	$r^2 = 0.649$
					$b = -11.118$	$p = 6.4E\text{-}55$		$\phi = -1.99$	$\phi = -0.0788$	$\phi = -2.73$	$p = 7.2E\text{-}07$
					$c = -0.023$			$\tau = 82.69$	$\tau = 15.6$	$\tau = 44.03$	
V1	*P. venosus*	A	Belau	51	$K = 7.303$	$r^2 = 0.998$		$a = 0.0972$	$a = 0.0766$	$a = 0.0631$	$r^2 = 0.516$
					$b = -12.15$	$p = 4.3E\text{-}68$		$\phi = 0.759$	$\phi = -2.87$	$\phi = 1.41$	$p = 1.2E\text{-}05$
					$c = -0.026$			$\tau = 180.3$	$\tau = 25.43$	$\tau = 17.73$	
V2	*P. venosus*	A	Belau	56	$K = 6.601$	$r^2 = 0.999$		$a = 0.07$	$a = 0.0871$	$a = 0.0747$	$r^2 = 0.597$
					$b = -12.576$	$p = 5.4E\text{-}83$		$\phi = -2.91$	$\phi = -3.13$	$\phi = -2.19$	$p = 3.2E\text{-}07$
					$c = -0.033$			$\tau = 58.29$	$\tau = 100.5$	$\tau = 117.2$	
V3	*P. venosus*	A	Belau	56	$K = 24.74$	$r^2 = 0.999$		$a = 0.169$	$a = 0.131$	$a = 0.0653$	$r^2 = 0.775$
					$b = -10.809$	$p = 5.4E\text{-}83$		$\phi = 2.83$	$\phi = 2.97$	$\phi = 2.87$	$p = 5.8E\text{-}14$
					$c = -0.02$			$\tau = 206.2$	$\tau = 342.9$	$\tau = 41.74$	
V4	*P. venosus*	A	Sesoko	39	$K = 703.605$	$r^2 = 0.986$		$a = 0.203$	$a = 0.131$	$a = 0.186$	$r^2 = 0.586$
					$b = -15.962$	$p = 2.4E\text{-}34$		$\phi = 1.16$	$\phi = 1.98$	$\phi = 2.21$	$p = 8.8E\text{-}05$
					$c = -0.012$			$\tau = 92.3$	$\tau = 30.56$	$\tau = 15.22$	
V5	*P. venosus*	A	Sesoko	29	$K = 0.315$	$r^2 = 0.996$		$a = 0.113$	$a = 0.0947$	$a = 0.0656$	$r^2 = 0.596$
					$b = -8.727$	$p = 8.4E\text{-}32$		$\phi = 0.614$	$\phi = -2.37$	$\phi = 2.26$	$p = 0.0084$
					$c = -0.042$			$\tau = 18.43$	$\tau = 87.76$	$\tau = 7.665$	
V6	*P. venosus*	A	Sesoko	60	$K = 11321.7$	$r^2 = 0.999$		$a = 0.0903$	$a = 0.0725$	$a = 0.061$	$r^2 = 0.515$
					$b = -17.365$	$p = 5.3E\text{-}86$		$\phi = 0.988$	$\phi = 2.78$	$\phi = -2.21$	$p = 6.4E\text{-}06$
					$c = -0.01$			$\tau = 114.3$	$\tau = 23.49$	$\tau = 190.9$	
V9	*P. venosus*	A	Sesoko	28	$K = 1.01$	$r^2 = 0.998$		$a = 0.116$	$a = 0.131$	$a = 0.102$	$r^2 = 0.789$
					$b = -18.108$	$p = 3.3E\text{-}34$		$\phi = 1.37$	$\phi = 2.53$	$\phi = 3.11$	$p = 0.00046$
					$c = -0.05$			$\tau = 47.95$	$\tau = 11.81$	$\tau = 16.66$	
V10	*P. venosus*	A	Sesoko	39	$K = 12948.2$	$r^2 = 0.997$		$a = 0.14$	$a = 0.0997$	$a = 0.0558$	$r^2 = 0.67$
					$b = -19.236$	$p = 4.7E\text{-}46$		$\phi = 3.05$	$\phi = -0.722$	$\phi = -3.02$	$p = 3.9E\text{-}06$
					$c = -0.011$			$\tau = 91.58$	$\tau = 17.31$	$\tau = 44.29$	
V11	*P. venosus*	A	Sesoko	20	$K = 3799.9$	$r^2 = 0.998$		$a = 0.066$	$a = 0.066$	$a = 0.056$	$r^2 = 0.65$
					$b = -17.033$	$p = 1.3E\text{-}20$		$\phi = 3.02$	$\phi = 1.26$	$\phi = -1.86$	$p = 0.039$
					$c = -0.016$			$\tau = 28.76$	$\tau = 7.51$	$\tau = 9.46$	
V12	*P. venosus*	A	Belau	53	$K = 1.839$	$r^2 = 0.999$		$a = 0.0701$	$a = 0.062$	$a = 0.0402$	$r^2 = 0.526$
					$b = -9.139$	$p = 1.8E\text{-}75$		$\phi = -2.35$	$\phi = 2.44$	$\phi = 2.62$	$p = 1.3E\text{-}06$
					$c = -0.036$			$\tau = 154.4$	$\tau = 65.21$	$\tau = 16.83$	
V13	*P. venosus*	A	Belau	60	$K = 2.24$	$r^2 = 0.999$		$a = 0.0893$	$a = 0.0794$	$a = 0.0776$	$r^2 = 0.454$
					$b = -13.024$	$p = 5.3E\text{-}86$		$\phi = 0.286$	$\phi = 0.362$	$\phi = 0.652$	$p = 7.1E\text{-}06$
					$c = -0.04$			$\tau = 63.68$	$\tau = 48.34$	$\tau = 19.5$	
V14	*P. venosus*	A	Belau	60	$K = 3.743$	$r^2 = 0.999$		$a = 0.0621$	$a = 0.0403$	$a = 0.0346$	$r^2 = 0.517$
					$b = -11.101$	$p = 5.3E\text{-}86$		$\phi = -0.297$	$\phi = 0.828$	$\phi = 0.338$	$p = 2.3E\text{-}07$
					$c = -0.028$			$\tau = 111.9$	$\tau = 19.11$	$\tau = 59.35$	
V15	*P. venosus*	A	Belau	61	$K = 2.69$	$r^2 = 0.999$		$a = 0.0651$	$a = 0.0431$	$a = 0.0354$	$r^2 = 0.411$
					$b = -11.477$	$p = 1.6E\text{-}87$		$\phi = 2.11$	$\phi = 1.4$	$\phi = 1.84$	$p = 0.0003$
					$c = -0.035$			$\tau = 198.9$	$\tau = 73.61$	$\tau = 18.04$	
V16	*P. venosus*	A	Belau	54	$K = 253.73$	$r^2 = 0.998$		$a = 0.0743$	$a = 0.598$	$a = 0.0436$	$r^2 = 0.539$
					$b = -13.18$	$p = 1.9E\text{-}69$		$\phi = -2.82$	$\phi = -2.87$	$\phi = 2.7$	$p = 7.1E\text{-}06$
					$c = -0.014$			$\tau = 240.9$	$\tau = 135.4$	$\tau = 17.97$	
V17	*P. venosus*	A	Belau	61	$K = 11.519$	$r^2 = 0.999$		$a = 0.0499$	$a = 0.0357$	$a = 0.0326$	$r^2 = 0.529$
					$b = -9.664$	$p = 1.6E\text{-}87$		$\phi = -2.85$	$\phi = -2.25$	$\phi = 2.31$	$p = 2.6E\text{-}07$
					$c = -0.02$			$\tau = 107.5$	$\tau = 38.44$	$\tau = 24.25$	
B1	*P. venosus*	B	Sesoko	80	$K = 11467$	$r^2 = 0.999$		$a = 0.113$	$a = 0.0996$	$a = 0.0782$	$r^2 = 0.476$
					$b = -17.676$	$p = 4.5E\text{-}119$		$\phi = -0.241$	$\phi = 1.46$	$\phi = 3.02$	$p = 5.5E\text{-}12$
					$c = -0.006$			$\tau = 1160$	$\tau = 346.1$	$\tau = 29.63$	
B2	*P. venosus*	B	Sesoko	97	$K = 29745$	$r^2 = 0.996$		$a = 0.0953$	$a = 0.0755$	$a = 0.0476$	$r^2 = 0.305$
					$b = -17.704$	$p = 1.3E\text{-}113$		$\phi = 1.08$	$\phi = 2.24$	$\phi = 0.0478$	$p = 2.8E\text{-}06$
					$c = -0.005$			$\tau = 519.1$	$\tau = 208.7$	$\tau = 26.41$	
B5	*P. venosus*	A	Sesoko	57	$K = 6.957$	$r^2 = 0.999$		$a = 0.0541$	$a = 0.0411$	$a = 0.0409$	$r^2 = 0.351$
					$b = -9.95$	$p = 1.7E\text{-}81$		$\phi = -1.62$	$\phi = 2.28$	$\phi = 2.6$	$p = 0.00074$
					$c = -0.027$			$\tau = 31.2$	$\tau = 65.45$	$\tau = 21.41$	
A1	*C. carpenteri*	A	Ishigaki-Jima	25	$K = 137$	$r^2 = 0.997$		$a = 0.131$	$a = 0.0635$	$a = 0.0674$	$r^2 = 0.522$
					$b = -8.709$	$p = 3.07E\text{-}31$		$\phi = 2.43$	$\phi = 1.69$	$\phi = 2.47$	$p = 0.011$
					$c = -0.025$			$\tau = 48.74$	$\tau = 7.135$	$\tau = 25.99$	
A2	*C. carpenteri*	A	Ishigaki-Jima	12	$K = 12.305$	$r^2 = 0.997$		$a = 0.0857$	$a = 0.0705$	$a = 0.0645$	$r^2 = 0.783$
					$b = -10.224$	$p = 1.2E\text{-}14$		$\phi = 1.97$	$\phi = 1.91$	$\phi = 2.74$	$p = 0.0494$
					$c = -0.114$			$\tau = 25.15$	$\tau = 9.266$	$\tau = 15.57$	

TABLE 1. Continued.

Specimen code	Taxon	A/B	Origin	Ch.	Gompertz parameter		Cycles			
A4	*C. carpenteri*	A	Ishigaki-Jima	24	$K = 2.594$	$r^2 = 0.994$	$a = 0.204$	$a = 0.156$	$a = 0.13$	$r^2 = 0.74$
					$b = -25.523$	$p = 1.2E-26$	$\phi = 0.934$	$\phi = 1.39$	$\phi = -0.112$	$p = 9.6E-04$
					$c = -0.134$		$\tau = 18.98$	$\tau = 25.15$	$\tau = 13.13$	
A7	*C. carpenteri*	A	Ishigaki-Jima	25	$K = 9968.8$	$r^2 = 0.986$	$a = 0.428$	$a = 0.333$	$a = 0.312$	$r^2 = 0.899$
					$b = -14.184$	$p = 1.5E-23$	$\phi = -1.69$	$\phi = 2.03$	$\phi = -1.98$	$p = 1.1E-05$
					$c = -0.015$		$\tau = 16$	$\tau = 26.56$	$\tau = 9.41$	
A9	*C. carpenteri*	A	Ishigaki-Jima	19	$K = 13.24$	$r^2 = 0.989$	$a = 0.348$	$a = 0.209$	$a = 0.147$	$r^2 = 0.851$
					$b = -8.047$	$p = 8.4E-19$	$\phi = 1.2$	$\phi = 1.48$	$\phi = 0.999$	$p = 5.1E-05$
					$c = -0.043$		$\tau = 26.08$	$\tau = 12.36$	$\tau = 74.48$	
A10	*C. carpenteri*	A	Ishigaki-Jima	23	$K = 57302$	$r^2 = 0.984$	$a = 0.342$	$a = 0.249$	$a = 0.194$	$r^2 = 0.8$
					$b = -13.712$	$p = 4.7E-21$	$\phi = 1.52$	$\phi = -3.13$	$\phi = -1.6$	$p = 1.7E-05$
					$c = -0.01$		$\tau = 62.72$	$\tau = 8.159$	$\tau = 23.97$	
A11	*C. carpenteri*	A	Ishigaki-Jima	24	$K = 114.65$	$r^2 = 0.998$	$a = 0.193$	$a = 0.117$	$a = 0.0947$	$r^2 = 0.66$
					$b = -9.542$	$p = 6.6E-32$	$\phi = 1.13$	$\phi = 2.52$	$\phi = 2.85$	$p = 0.0008$
					$c = -0.03$		$\tau = 26.09$	$\tau = 15.41$	$\tau = 10.72$	

power functions of equations (4) and (5)

$$t = (i/2.849)^{1.965} \tag{6}$$

for *P. venosus* gamonts/schizonts and

$$t = (i/1.289)^{1.433} \tag{7}$$

for *C. carpenteri*.

Concerning the chamber-building rate for agamonts (B-forms), literally no data are available in the literature. Most of the information pertains to general estimations of lifetime only as derived from population dynamics (Hohenegger 2006), bauplan structure (Ferràndez-Cañadell 2012), or isotopic studies (Purton and Brasier 1999). Mathematical representations of the agamonts' chamber-building rate can be made by using gamonts' data, increasing the chamber-building rate for the initial part with the smallest chambers and relating it to lifetime estimation. Most probably, however, differences in chamber form between agamonts and gamonts/schizonts would result in quite different chamber-building rates for the two generations. In fact, agamonts possibly grow faster than the gamonts/schizonts at the beginning, then, owing to their extreme K-strategy biological adaptations, reduce their growth speed. We have therefore modified the data published by Krüger (1994) on the gamonts to obtain two growth functions to simulate a maximum lifetime of two and three years.

The functions we used are therefore expressed as

$$i = 4.45t^{0.442} \tag{8}$$

for the three-year estimated lifetime and

$$i = 5.5t^{0.442} \tag{9}$$

for the two-year estimated lifetime.

Cyclicity was checked on the standardized residuals (eq. 3) by power spectral analysis using both Lomb periodogram (Press et al. 1992) and REDFIT spectral analysis (Schulz and Mudelsee 2002). Furthermore, to visualize how these cycles fit the obtained volume residuals, we calculated the sum of the three most significant sinusoidal functions for each specimen to obtain amplitudes a and phases ϕ of sinusoidal functions with given periods τ. These analyses are shown for specimen V4 of the data set in Figure 3.

The frequency distribution reveals significant periods during the lifetime of *P. venosus* gamont/schizonts. If all periods are weighted equally, then period τ for the k^{th} cycle of specimen j is described by the following function,

$$f(\tau_{jk}) = 1. \tag{10}$$

However, because of different lifetimes expressed in chamber number and differing amplitude values, the period τ_{jk} should be weighted based on chamber numbers n_j and amplitudes a_{jk} :

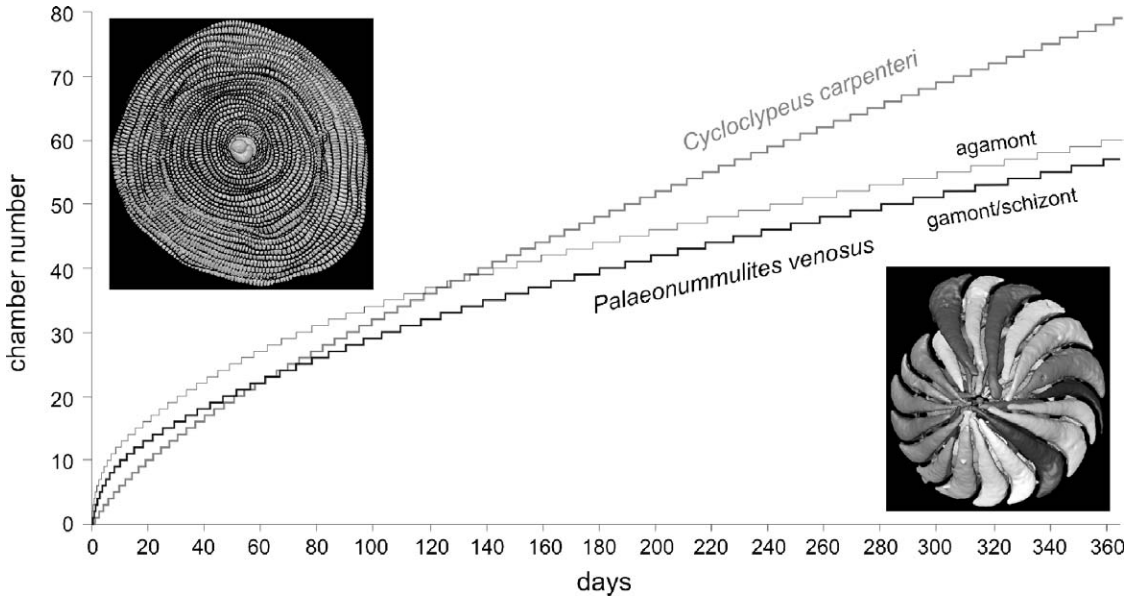

FIGURE 2. Estimated growth functions from literature data for *Palaeonummulites venosus* using equation (4) for gamonts/schizonts and equation (8) for agamonts, and *Cycloclypeus carpenteri* using equation (5). Lower right: 3-D rendered model of specimen V14, maximum diameter 2.6 mm. Upper left: 3-D rendered model of specimen A1, maximum diameter 7.6 mm.

$$f(\tau_{jk}) = a_{jk}\, n_j. \tag{11}$$

Amplitudes of periods are the main factor in this weighting, additionally strengthened by multiplication with chamber number.

When the resulting frequency histogram of weighted periods is strictly inhomogeneous, this confirms concentration centers around distinct and significant periods, whereas a homogeneous distribution would argue against significant periods. This can be checked by decomposing the frequency distribution into normal-distributed components. Decomposition into components was done by nonlinear regression (Fig. 4).

Segmentation and extraction of chambers on the three-dimensional models was done with the image software Amira 5.4.3 by VSG; parameters of the Gompertz function and the decomposition into components was run with PAWS statistic v.18.0; power spectral analyses and sinusoidal functions were performed with PAST v. 2.17b (Hammer et al. 2001), and basic calculation with Microsoft Office Excel 2003.

Results

The significant cycles with amplitudes a, phases ϕ, and periods τ are reported in Table 1 for every specimen. Significant periods were obtained by REDFIT functions, applying the highest oversampling (4) to increase the number of points through spectral analysis. Only points possessing power above the 90% χ^2 false alarm level were selected and included in the calculation.

For *P. venosus* gamonts/schizonts, the histogram based on weighted frequencies shows concentrations around specific periods (Fig. 4). Decomposition into normal-distributed components resulted in five significant components with narrow standard deviations (Table 2); there is minimal overlapping between component distributions (Fig. 4), as confirmed by the gap between upper and lower 5% confidence limits for the mean of neighboring components. This strongly confirms significant periods.

The period found the greatest proportion of specimens has a mean length of 13.3 days, followed by that with a mean length of 88.4 days (Table 2). Periods with mean lengths of

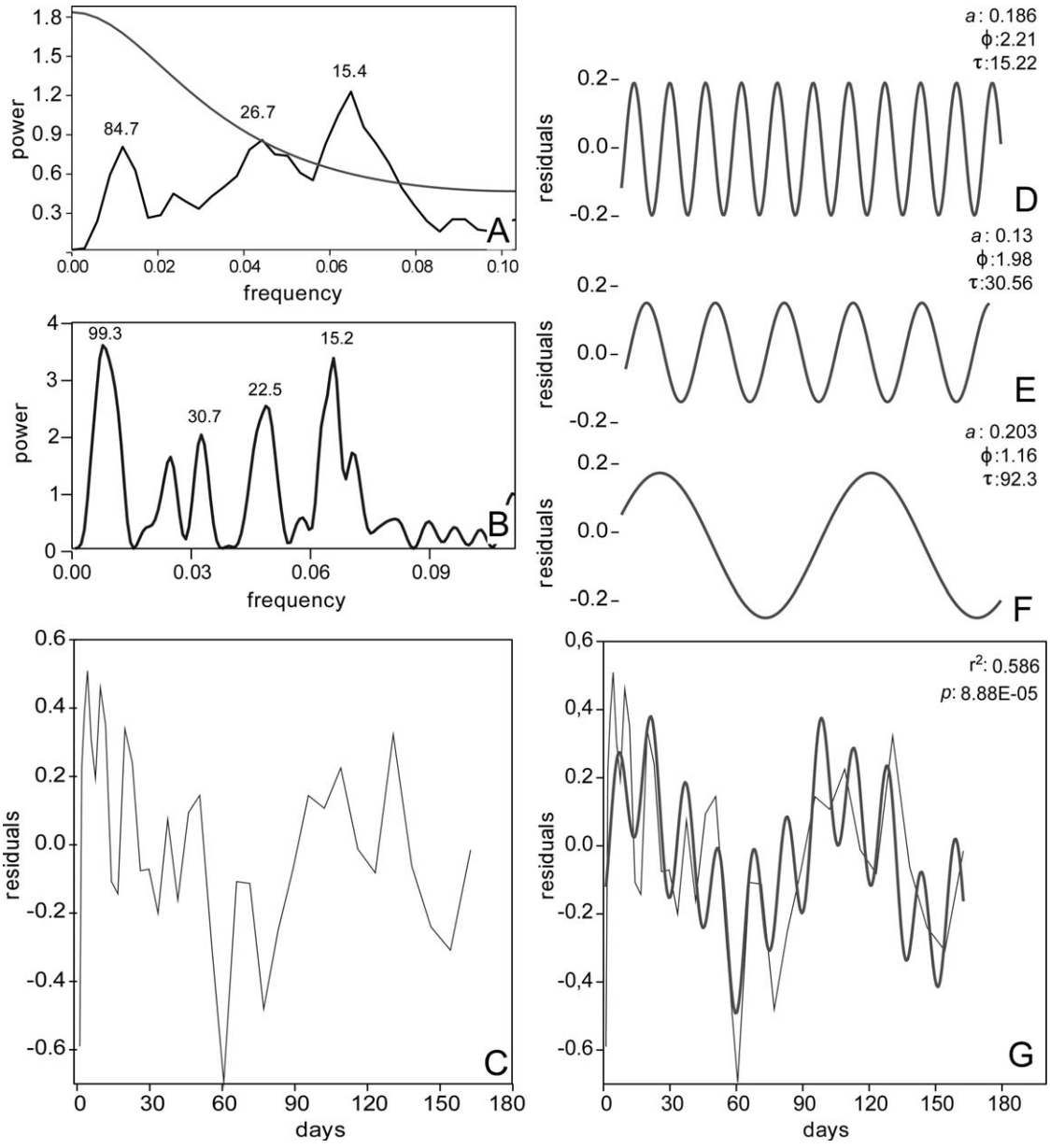

FIGURE 3. Cyclicity results for one specimen (V4). A, REDFIT spectral analysis with the most significant periods. The curved line represents the false alarm line for 90% χ^2 parametric approximation. B, Lomb periodogram with the main prominent periods. C, Standardized and linearized residuals of growth deviations (obtained by eq. 3) with respect to time. D–F, The three most significant cycles to model growth oscillation of the 39 segmented chambers. G, Results of this analyses, with the three most significant cycles plotted over the calculated residuals. The quality of fit for only these three cycles is determined by the coefficient of determination r^2 together with the probability of non-correlation p.

28.6, 48.3, and 62.7 days are of lesser, but similar importance.

When *P. venosus* gamont/schizonts are separated by location, the frequency distributions show slight differences (Fig. 5). Specimens from Sesoko-Jima possess significant mean periods of 13.9, 29.9, and 88.4 days that strongly correspond to lunar cycles and seasons. Significant periods in specimens from Belau peak at 9.0 and 19.8 days, followed by mean period lengths of 64.1 days, 202.4 days, and 342.9 days (Fig. 5). The two shortest periods observed in

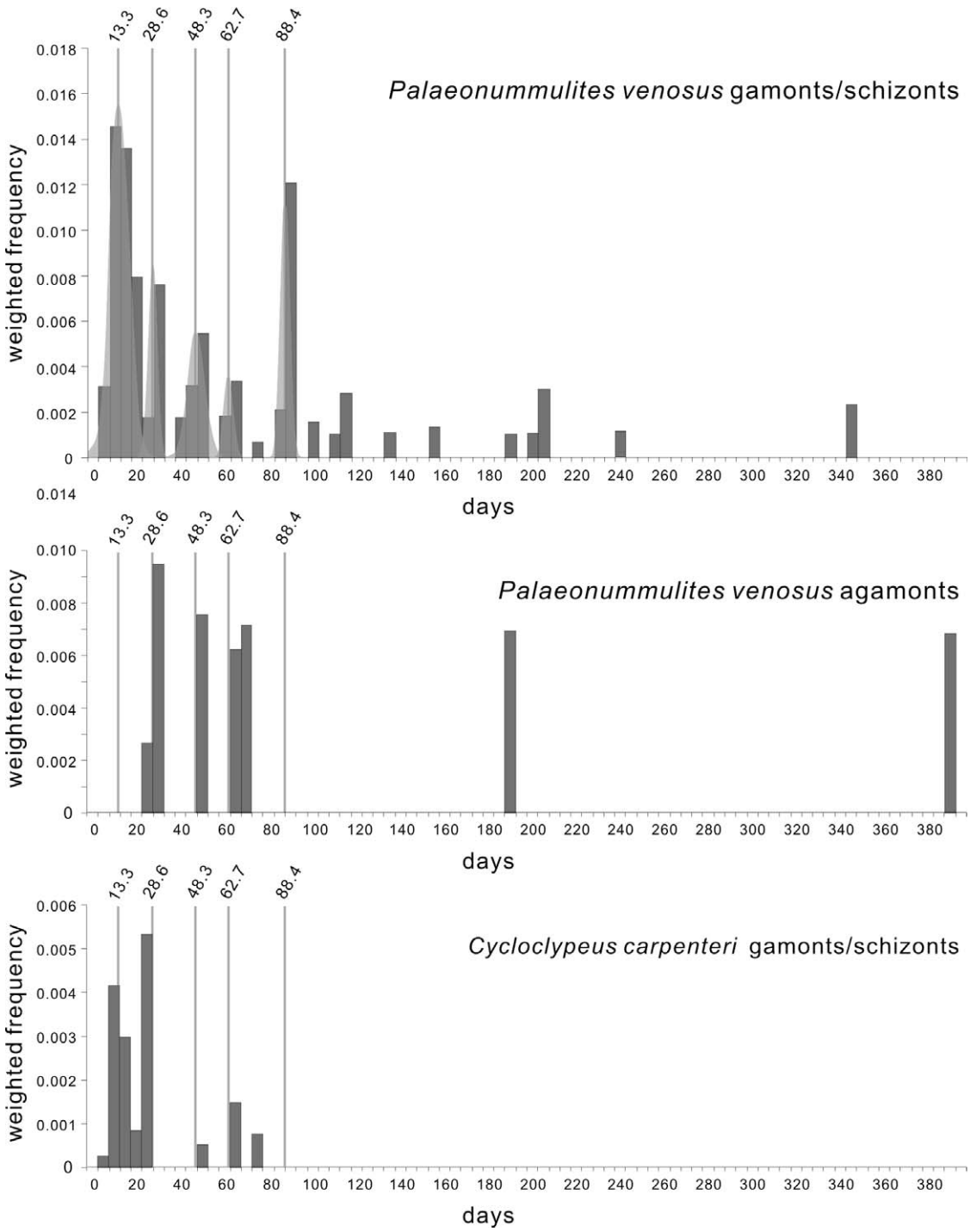

FIGURE 4. Histograms of most significant cycles for the investigated specimens.

the Belau specimens do not seem to correspond to any constant environmental variation. They could point to tidal cycles only if a multiplication factor of 1.5 is included; the other cycles have periods that approximate two months, half a year, and one year.

Differences in weighted frequencies between Sesoko Jima and Belau (Fig. 5) are not

TABLE 2. Parameters of the five significant periods in sinusoidal oscillations of Palaeonummulites venosus gamonts/schizonts.

Significant periods	Mean in days	Standard deviation	Percentage	5% confidence limits	
				Lower	Upper
1	13.3	5.2	49.0	3.1	23.5
2	28.6	1.4	10.5	25.9	31.3
3	48.3	2.8	11.0	42.8	53.8
4	62.7	1.4	9.6	60.0	65.5
5	88.4	1.5	20.0	85.3	91.2

correlated with differences in numbers of specimens (8 and 9) or numbers of chambers (Sesoko: mean = 39.5, SD = 13.4; Belau: mean = 56.9, SD = 3.6) but on amplitude (Sesoko: mean = 0.093, SD = 0.043; Belau: mean = 0.068, SD = 0.030). Whereas differences in chamber numbers are artificial, because they depend on the particular specimens selected for the investigation, differences in amplitude between Sesoko and Belau are inherent and highly significant, with the probability of concordance $p(H_0) = 0.009$.

Using the three-year lifetime (eq. 8) of the two investigated agamonts of *P. venosus* from Sesoko Jima, which build more chambers than the gamonts/schizonts and attain larger size, the most significant cycles with means of 28.4, 51.0, and 67.1 days are similar to those seen in the gamonts/schizonts, except for the lack of the 13.3-day cycles and the presence of very long cycles at 191.2 and 390.8 days (Fig. 4). The cycles with period length of 28.4 and 51.0 days fall exactly within the 5% confidence limits of the second and third period in gamonts/schizonts, while the period of 67.1 days is positioned a little bit above the upper 5% limit of the fourth significant period in gamonts/schizonts (Table 2). Using equation (9) for the chamber-building rate characterizing a two-year lifetime of agamonts, the significant periods become exactly half of those assuming a three-year lifetime,

In *C. carpenteri* gamonts/schizonts the chamber volumes show significant cycles of 12.4-day and 25.6-day periodicity (Fig. 4). The periods of 48.7 and 68.0 days are much less significant. All periods are positioned within the 5% confidence limits of the corresponding periods of *P. venosus* gamonts/schizonts (Table 2).

Discussion

The results clearly show consistent cyclicity in all investigated specimens of *P. venosus* and *C. carpenteri*, which can be interpreted by the above-mentioned fluctuations. Gamonts/schizonts of both species and agamonts of *P. venosus* show growth oscillations that are well represented by sinusoidal functions defined by comparable periods. Depending on the lifetime of these organisms, the number of chambers per time unit causes significant variation in cycle periods. According to the ontogeny proposed here, building many chambers per time interval, as in all gamonts/schizonts and the agamonts with the two-year lifetime, leads to the observation of short-period cycles. For long-lived organisms (i.e., agamonts with a three-year lifetime estimation), the shortest cycles are not evident because the data over the long lifetime interval are insufficient for resolving cycles with shorter periods.

Nonetheless, similar periodicities occur for all chamber-building rates and for all investigated specimens. In fact, oscillations with period lengths around 13.3 days and between 26 and 31 days are the most common and most significant for all investigated specimens in both generations.

Possible explanations for these periodicities might be found in very short orbital cycles such as tidal and lunar ones (Fig. 6). Lunar-cycle-associated physiology has long been known in a wide variety of organisms (Naylor 1982). Although it is most commonly documented in land plants and shallow-water taxa, even deep-water metazoans are now known to be moonlight dependent (Mercier et al. 2011). It is therefore not surprising that LBF growth (in all its stages) is affected by light

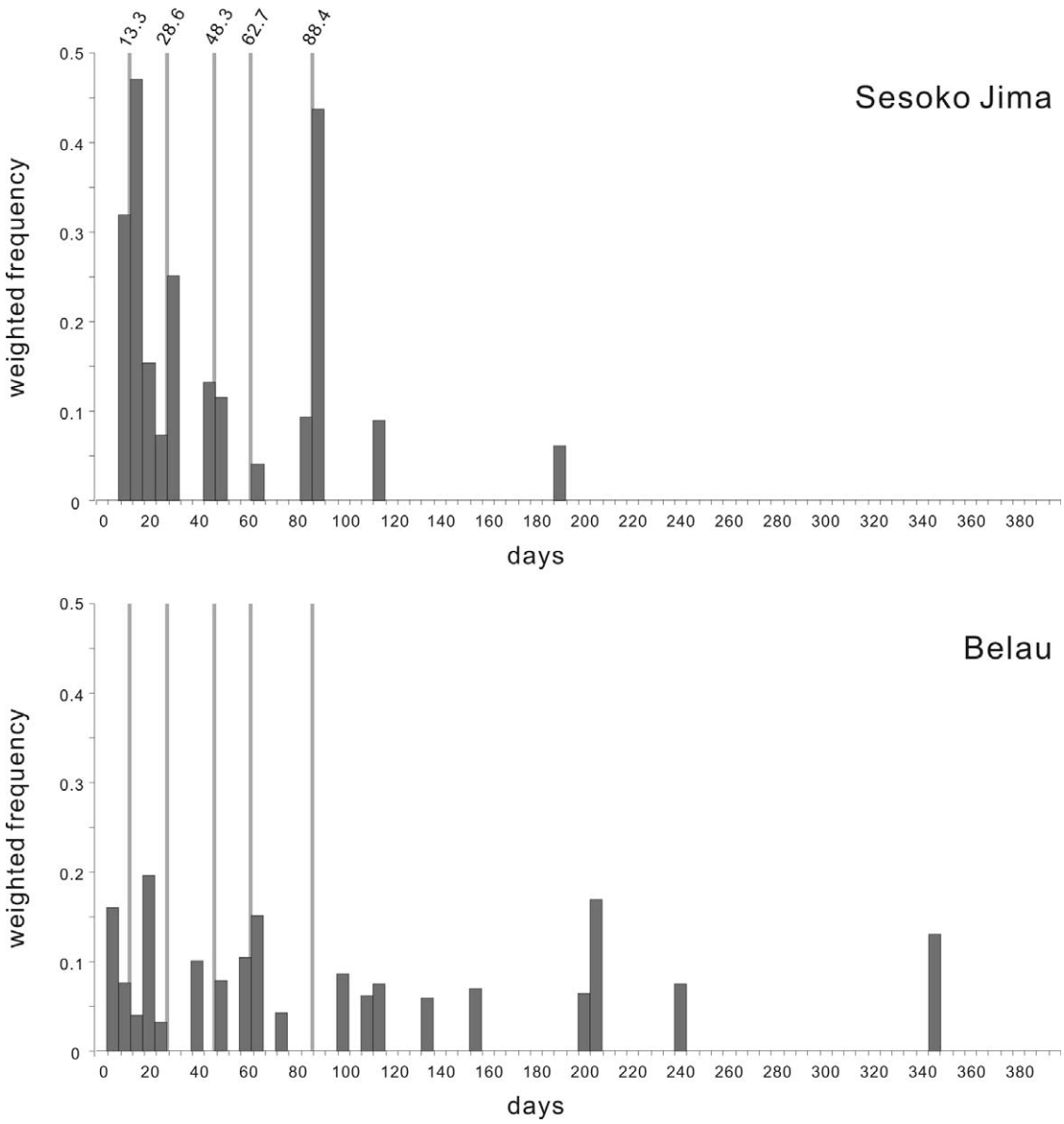

FIGURE 5. Histograms of most significant cycles weighted by amplitudes for the investigated specimens by locality.

intensity. Moon-dependent reproductive cycles have also been observed in planktic foraminifera (Bijma et al. 1990 and reference therein), and Rigual-Hernández et al. (2012) has reviewed several possible implications by these results.

So far, light dependence on LBF has only been confirmed as an important factor affecting the general shape of foraminiferal tests (Hohenegger 2009 and references therein); its influence on chamber size variation during ontogeny has been neither observed nor measured. Therefore, the significant cycles we observed with period lengths between 25.9 and 31.3 days possibly reflect the influence of full-moon light intensity.

Even if clear evidence for a correlation between moon light intensity and foraminifera can be explained by the presence of photosymbiotic algae hosted by the foraminifera, an explanation for the correlation between tidal

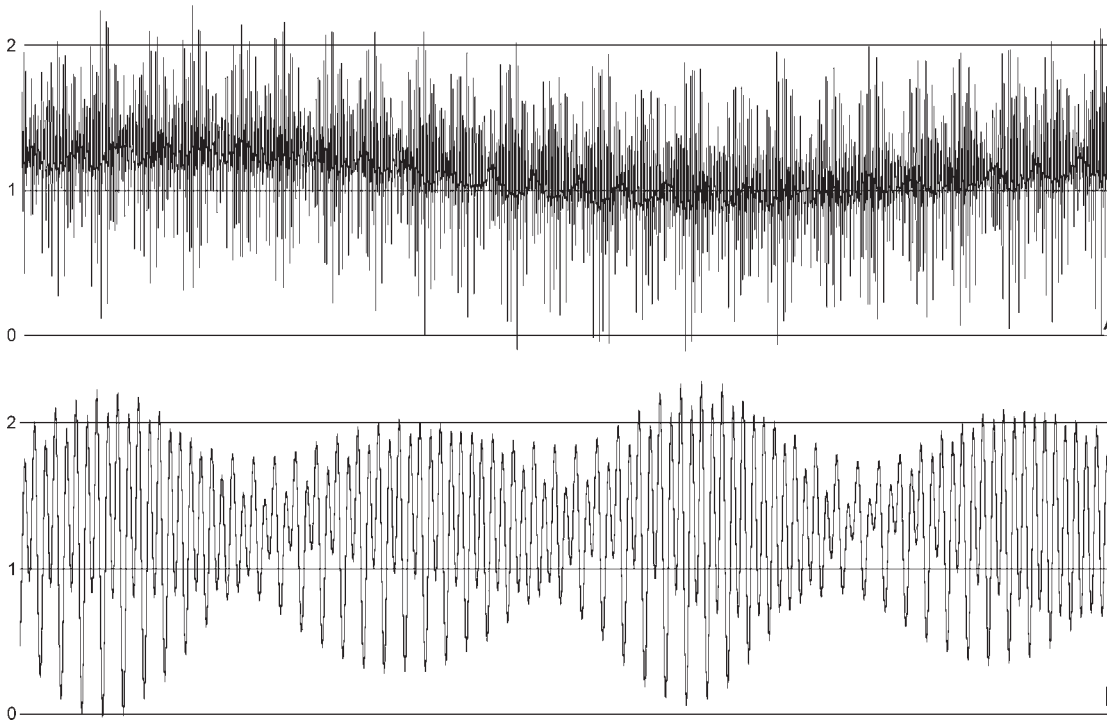

FIGURE 6. Tidal charts for Toguchi (Okinawa, Japan); heights are given in meters. A, One-year chart. B, Two-month chart. Source: http://tbone.biol.sc.ed.

cycles and foraminiferal growth is harder to find and subject to more speculation.

Larger foraminifera are known to be oligotrophic organisms; they need a minimal food supply and are restricted to the photic zone of warm-water environments (Hottinger 1997, 2000). They must therefore be adapted to all those factors affecting such an environment, such as tidal forces, light intensity, strong variation in water motion, and temperature fluctuation.

In the region where the samples were collected (Okinawa and Belau), tides have a semi-diurnal range, where the difference in height between high and low water spans half a day (Fig. 6). Semi-diurnal tides have a periodicity of twice per lunar month. Perfectly aligned with the new moon and full moon are two major heights of water, the spring tides. Spring tides result in waters that are higher than average high waters and lower than the average low waters. This phenomenon has an oscillation period of 14 days, visible in the investigated foraminifera.

Tidal cycles with very high peaks, such as the 2-m-high tides seen at Okinawa Island, can produce very strong tidal currents that run at the water sediment interface and can reach very deep environments (Zuo et al. 2009). Larger foraminifera, with their semi-sessile benthic lifestyle are somehow affected not by the tidal current itself, but possibly by the differences in currents caused by neap and spring tides. Tidal currents, as they run close to the water-sediment interface, are able to put into suspension a large amount of fine sediment, thus decreasing water clarity but also increasing the availability of inorganic nutrients, which the foraminifera need for their symbionts.

Strong changes in water temperature from a minimum of 19° in February to a maximum of 27.5° at 50-m depth of the sampling location (Hohenegger 2004: Fig. 5B) may cause oscillations with period lengths of one year. Besides these very long-period oscillations as observed in the B generation, tides also possess

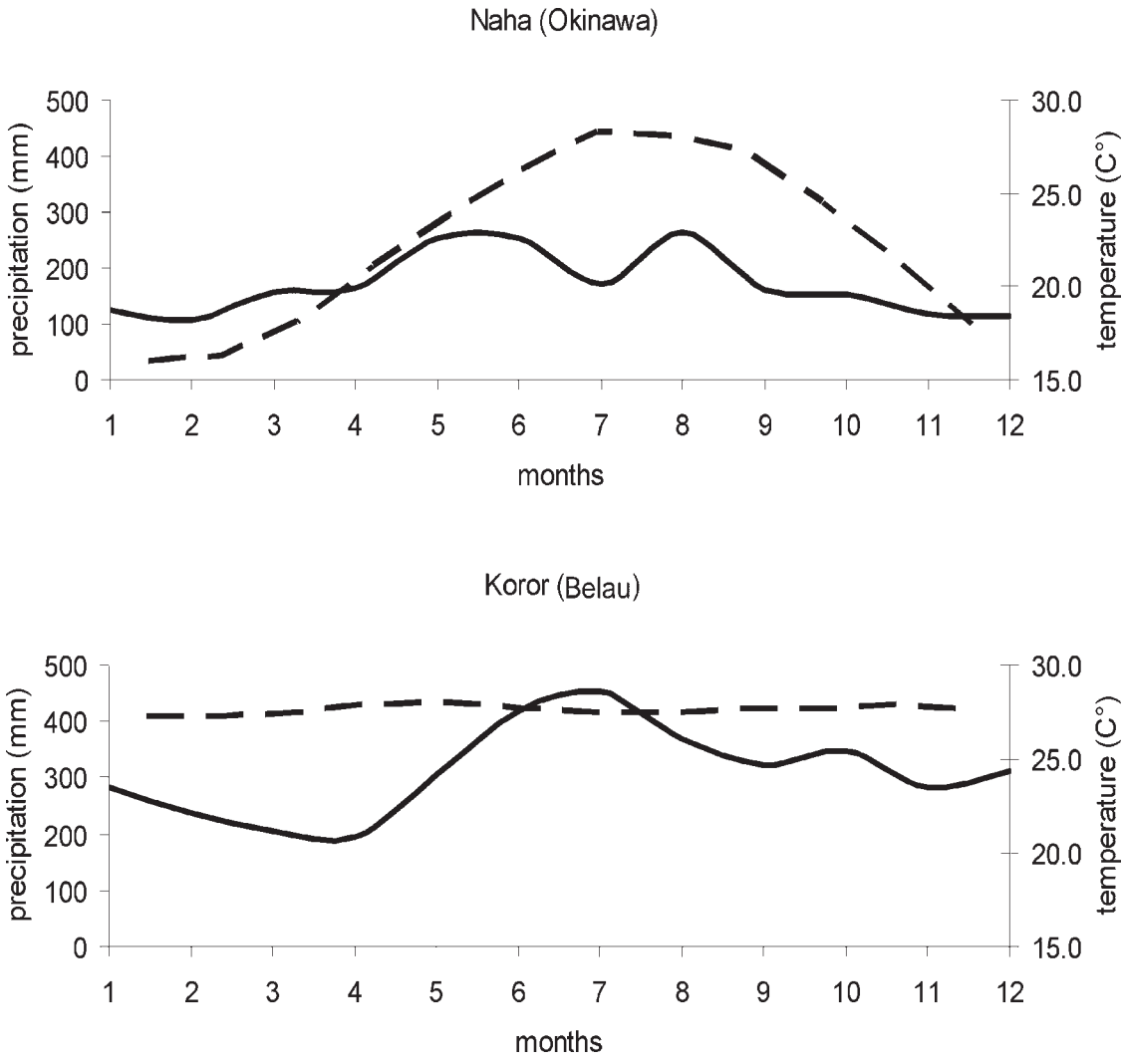

FIGURE 7. Precipitation (solid line) and temperature (dashed line) diagram for Okinawa (A) and Belau (B).

a very long cyclicity, which fits very well with the one-year cycle (Fig. 6).

Furthermore, latitude apparently might also affect oscillations. In fact, some differences in significant cycles are visible between the specimens collected at the Tropic of Cancer (Sesoko-Jima) and those collected near the equator (Belau). The climate of Sesoko-Jima, where the monsoon front crosses the Ryukyu Archipelago in June and re-crosses in September/October, is expressed in two strong rainy seasons (Fig. 7A). Winter starts with cooler temperatures in December and finishes in February. This could explain the significant period length of 88.4 days for the gamonts/schizonts, representing a 3-month cycle. The higher latitudinal position of the Ryukyu archipelago could explain the greater influence of spring tides at the new and full moon (13.9 days and 29.9 days) (Hohenegger and Briguglio 2014).

Being located close to the equator (Fig. 1) Belau has no seasons, but it has more intense rainfall, which peaks at the summer solstice, followed by a lower peak at the autumn equinox and a third, again slightly lower, peak at the winter solstice (Fig. 7B). Tidal cycles are much less prominent in these samples (Fig. 5B) and it seems that there is no significant difference between new-moon and full-moon spring tides. Furthermore, Hallock (1981)

observed that the growth rates of *Amphistegina lessonii* and *A. lobifera* from Belau are twice those from Hawaii; therefore it is possible that the two significant peaks observed at 9.0 and 19.8 days were caused by erroneous estimates of growth rate for Belau individuals. If we modify the growth rate by a factor of 1.5, the new peaks are at 14.0 and 30.8 days, again representing the new- and full-moon phases.

The cycle with a period of 202.4 days could be interpreted as the half-year cycle corresponding to the rainy peaks in summer and winter. Furthermore, the significantly lower amplitudes in all cycles relative to those at Sesoko Jima are additional demonstrations of life near the equator with consistent climatic conditions, only weakly affected by seasonal changes.

Conclusion

Larger foraminifera can be considered as unique minute archives composed of many sequential registrations (as large as the number of chambers) of the environmental conditions present during the individual's lifetime. A variety of environmental changes may be visible in size and shape of the chamber. Depending on the chamber-building rate, which follows the Michealis-Menten function (Hohenegger and Briguglio 2014) and is approximated by the power functions in this article, the particular cycles or variations may or may not be visible. For short cycles or variations to be registered, a fast chamber-building rate is necessary, whereas long-term cycles require that the lifetime be at least as long as the cycle needs to repeat itself.

Our use of computed tomography on several specimens of larger benthic foraminifera and the quantification of the volume of all their chambers has made it possible to quantify the growth of these single cells. From our results, we can confirm that the growth of larger benthic foraminifera is affected by lunar cycles that change the intensity of tidal currents and availability of moonlight. These cycles influence environmental factors such as water turbidity, nutrient availability, and light intensity. Because all these types of information, as presented here, are registered in test growth, it will also be possible to investigate with great accuracy the evolution of such parameters in the past, when similar cyclicity can be found in fossil material.

Even if further studies on the chamber-building rate for the recent species are needed in order to get better cycle resolution and more stable growth parameters, the preliminary results presented here clearly identify the larger foraminifera as a group of protists whose functional morphology is perfectly adapted to their environment. The study of their test morphology and how it changes during ontogeny is the best way to interpret environmental factors acting on the specimen during its lifetime.

In the future, it may be possible to run the analyses here reported on simultaneously collected living individuals from different environments; this would allow a unique opportunity to synchronize the cycles among the specimens and possibly to observe how cohorts (i.e., populations) of LBF react to identical environmental changes and how they grow and move through time together.

Acknowledgments

This work was developed within the project "Functional Shell Morphology of Larger Benthic Foraminifera" of the Austrian Science Fund (FWF; grant P23459-B17). We thank the Institute of Palaeontology, University of Vienna, for letting us scan the majority of the presented specimens and for providing a dedicated working station for analyzing the data sets. We thank G. Müller and B. Metscher (Department of Theoretical Biology, University of Vienna) for letting us use the nanoCT for specimens V0. The help of W. Fabienke to segment some of the specimens is also highly appreciated. The constructive comments of R. Lewis and J. Tyszka greatly improved the manuscript.

Literature Cited

Barker, S., I. Cacho, H. Benway, and K. Tachikawa. 2005. Planktonic foraminiferal Mg/Ca as a proxy for past oceanic temperatures: a methodological overview and data compilation for the Last Glacial Maximum. Quaternary Science Reviews 24:821–834.

Batschelet, E. 1971. Introduction to mathematics for life scientists. Springer, Berlin.

Beavington-Penney, S. J., and A. Racey. 2004. Ecology of extant nummulitids and other larger benthic foraminifera: applications

in palaeoenvironmental analysis. Earth-Science Reviews 67:219–265.

Benedetti, A., and A. Briguglio. 2012. *Risananeiza crassaparies* n. sp. from the Late Chattian of Porto Badisco (southern Apulia). Bollettino della Società Paleontologica Italiana 51:167–176.

Bijma, J., J. Erez, and C. Hemleben. 1990. Lunar and semi-lunar reproductive cycles in some spinose planktonic foraminifers. Journal of Foraminiferal Research 20:117–127.

Briguglio, A., and A. Benedetti. 2012. X-ray microtomography as a tool to present and discuss new taxa: the example of *Risananeiza* sp. from the late Chattian of Porto Badisco. Rendiconti Online Società Geologica Italiana 21:1072–1074.

Briguglio, A., and J. Hohenegger. 2009. Nummulitids hydrodynamics: an example using *Nummulites globulus* Leymerie, 1846. Bollettino della Società Paleontologica Italiana 48:105–111.

———. 2011. How to react to shallow water hydrodynamics: the larger benthic foraminifera solution. Marine Micropaleontology 81:63–76.

Briguglio, A., B. Metscher, and J. Hohenegger. 2011. Growth rate biometric quantification by x-ray microtomography on larger benthic foraminifera: three-dimensional measurements push nummulitids into the fourth dimension. Turkish Journal of Earth Science 20:683–699.

Briguglio, A., J. Hohenegger, and G. Less. 2013. Paleobiological applications of three-dimensional biometry on larger benthic foraminifera; a new route of discoveries. Journal of Foraminiferal Research 43:67–82.

Briguglio, A., J. Wöger, E. Wolfgring, and J. Hohenegger. 2014. Changing investigation perspectives: methods and applications of computed tomography on Larger Benthic Foraminifera. Pp. 55–70 *in* Kitazato and Bernhard 2014.

Dettmering, C., R. Röttger, J. Hohenegger, and R. Schaljohann. 1998. The trimorphic life cycle in foraminifera: observations from cultures allow new evaluation. European Journal of Protistology 34:363–368.

Egger, H., A. Briguglio, F. Rögl, and R. Darga. 2013. The basal Lutetian Transgression on the Tethyan shelf of the European craton (Adelholzen formation, Eastern Alps, Germany). Newsletter of Stratigraphy 46:287–301.

Evans, D., W. Müller, S. Oron, and W. Renema. 2013. Eocene seasonality and seawater alkaline earth reconstruction using shallow-dwelling large benthic foraminifera. Earth and Planetary Science Letters 381:104–115.

Ferràndez-Cañadell, C. 2012. Multispiral growth in *Nummulites*: paleobiological implications. Marine Micropaleontology 97:105–122.

Fraile, I., S. Mulitza, and M. Schulz. 2009. Modeling planktonic foraminiferal seasonality: implications for sea-surface temperature reconstructions. Marine Micropaleontology 72:1–9.

Fulton, T. W. 1901. The rate of growth of the cod, haddock, whiting, and Norway pout. Pp. 154–228 *in* Nineteenth Annual Report of the Fishery Board for Scotland, Part II.

Gebhardt, H., S. Ćorić, R. Darga, A. Briguglio, B. Schenk, W. Werner, N. Andersen, and B. Sames. 2013. Middle to Late Eocene paleoenvironmental changes in a marine transgressive sequence from the northern Tethyan margin (Adelholzen, Germany). Austrian Journal of Earth Science 106:45–72.

Görög, A., B. Szinger, E. Toth, and J. Viszkok. 2012. Methodology of the micro-computer tomography on foraminifera. Palaeontologia Electronica 15(1), art. 3T.

Hallock, P. 1981. Production of carbonate sediments by selected large benthic foraminifera on two Pacific coral reefs. Journal of Sedimentary Petrology 51:467–474.

———. 1985. Why are larger foraminifera large? Paleobiology 11:195–208.

Hammer, Ø., D. A. T. Harper, and P. D. Ryan. 2001. PAST: Paleontological statistics software package for education and data analysis. Palaeontologia Electronica 4(4), art. 1. http://palaeo-electronica.org/2001_1/past/issue1_01.htm.

Hohenegger, J. 1996. Remarks on the distribution of larger foraminifera (Protozoa) from Belau (Western Carolines). Kagoshima University Research Center for the South Pacific, Occasional Papers 30:85–90.

———. 2004. Depth coenoclines and environmental considerations of western pacific larger foraminifera. Journal of Foraminiferal Research.34:9–33.

———. 2006. The importance of symbiont-bearing benthic foraminifera for West Pacific carbonate beach environments. Marine Micropaleontology 61:4–39.

———. 2009. Functional shell geometry of symbiont-bearing benthic foraminifera. Galaxea 11:1–9.

Hohenegger, J., and A. Briguglio. 2012 Axially oriented sections of nummulitids: a tool to interpret larger benthic foraminiferal deposits. Journal of Foraminiferal Research 42:145–153.

———. 2014. Methods for estimating growth pattern and lifetime of foraminifera based on chamber volumes. Pp. 29–54 *in* Kitazato and Bernhard 2014.

Hohenegger, J., E. Yordanova, Y. Nakano, and F. Tatzreiter. 1999. Habitats of larger foraminifera on the upper reef slope of Sesoko Island, Okinawa, Japan. Marine Micropaleontology 36:109–168.

Hohenegger J., A. Briguglio, and W. Eder. 2014. The natural laboratory of symbiont-bearing benthic foraminifera Studying individual growth and population dynamics in the sublittoral. Pp. 13–28 *in* Kitazato and Bernhard 2014.

Hottinger, L. 1982. Larger foraminifera, giant cells with a historical background. Naturwissenschaften 69:361–371.

———. 1997. Shallow benthic foraminiferal assemblages as signals for depth of their deposition and their limitations. Bulletin de la Société Géologique de France 168:491–505.

———. 2000. Functional morphology of benthic foraminiferal shells, envelopes of cells beyond measure. Micropaleontology 46:57–86.

———. 2006. Illustrated glossary of terms used in foraminiferal research. Notebooks of Geology 2006/2:1–4. http://paleopolis.rediris.es/cg/CG2006_M02/index.html.

King, A., and W. R. Howard. 2005. δ18O seasonality of planktonic foraminifera from Southern Ocean sediment traps: latitudinal gradients and implications for paleoclimate reconstructions. Marine Micropaleontology 56:1–24.

Kitazato, H., and J. Bernhard, eds. 2014. Experimental approaches in foraminifera: collection, maintenance, and experimentation. Springer Japan (Environmental Science Series), Osaka.

Kosuge, T., H. Shimizu, and K. Yano. 1997. What can we find in the fore reef area? Dredging results in coastal waters of Ihigaki Jima. Research Station for the Western Sea (Nishi Kai Sui Ken). News 19:6–9. [In Japanese.]

Krüger, R. 1994. Untersuchungen zum Entwicklungsgang rezenter Nummulitiden: *Heterostegina depressa*, *Nummulites venosus* und *Cycloclypeus carpenteri*. Ph.D. thesis. Christian-Albrechts-Universität, Kiel.

Lietz, R. 1996. Untersuchungen zur Individualentwicklung der Groforaminifere *Cycloclypeus carpenteri* Carpenter (1856). Master's thesis. Institut für Allgemeine Mikrobiologie an der Christian-Albrechts- Universität, Kiel.

Mercier, A., Z. Sun, S. Baillon, and J. F. Hamel. 2011. Lunar rhythms in the deep sea: evidence from the reproductive

periodicity of several marine invertebrates. Journal of Biological Rhythms 26:82–86.

Naylor, E. 1982. Tidal and lunar rhythms in animals and plants. *In* J. Brady, ed. Biological timekeeping. Society of Experimental Biology Seminar Series 14:33–48.

Olsson, R. K. 1973. What is a kummerform planktonic foraminifer? Journal of Paleontology 47:327–329.

Press, W. H., S. A. Teukolsky, W. T. Vetterling, and B. P. Flannery. 1992. Numerical recipes. Cambridge University Press, Cambridge.

Purton, L. M. A., and M. D. Brasier. 1999. Giant protist *Nummulites* and its Eocene environment: life span and habitat insights from $\delta^{18}O$ and $\delta\ ^{13}C$ data from *Nummulites* and *Venericardia*, Hampshire basin, UK. Geology 27:711–714.

Rigual-Hernández, A. S., F. J. Sierro, M. A. Bárcena, J. A. Flores, and S. Heussner. 2012. Seasonal and interannual changes of planktic foraminiferal fluxes in the Gulf of Lions (NW Mediterranean) and their implications for paleoceanographic studies: two 12-year sediment trap records. Deep-Sea Research Part I: Oceanographic Research Papers 66:26–40.

Röttger, R. 1972. Analyse von Wachstumskurven von *Heterostegina depressa* (Foraminifera: Nummulitidae). Marine Biology 17:228–242.

———. 1990. Biology of larger foraminifera: present status of the hypothesis of trimorphism and ontogeny of the gamont of *Heterostegina depressa*. Pp. 43–54 *in* Y. Takyanagi and T. Saito, eds. Studies in benthic foraminifera: Benthos '90. Proceedings of the Fourth International Symposium on Benthic Foraminifera. Tokai University Press, Sendai.

Röttger, R., and M. Spindler. 1976. Development of *Heterostegina depressa* individuals (Foraminifera, Nummulitidae) in laboratory cultures. *In* C. T. Shafer and B. R. Pelletier, eds. First international symposium on benthonic foraminifera of continental margins, Part A, ecology and biology. Maritime Sediments Special Publication 1:81–87.

Schmidt, D. N., E. J. Rayfield, A. Cocking, F. Marone. 2013. Linking evolution and development: synchrotron radiation X-ray tomographic microscopy of planktic foraminifers. Palaeontology 56:741–749.

Schulz, M., and M. Mudelsee. 2002. REDFIT: estimating red-noise spectra directly from unevenly spaced paleoclimatic time series. Computers and Geosciences 28:421–426.

Serra-Kiel, J., L. Hottinger, E. Caus, K. Drobne, C. Ferrandez, A. K. Jauhri, G. Less, R. Pavlovec, J. Pignatti, J. M. Samso, H. Schaub, E. Sirel, A. A., Strougo, Y. Tambareau, J. Tosquella, and E. Zakrevskaya. 1998. Larger foraminiferal biostratigraphy of the Tethyan Paleocene and Eocene. Bulletin de la Société Géologique de France 169:281–299.

Speijer, R. P., D. Van Loo, B. Masschaele, J. Vlassenbroeck, V. Cnudde, and P. Jacobs. 2008. Quantifying foraminiferal growth with high-resolution X-ray computed tomography: new opportunities in foraminiferal ontogeny, phylogeny, and paleoceanography applications. Geosphere 4:760–763.

Tyszka, J. 2004. Analysis of test ontogenesis (ATO) in small foraminifera: implications from *Pseudonodosinella*. *In* M. A. Kaminsky and R. Coccioni, eds. Proceedings of the Sixth International Workshop on Agglutinated Foraminifera, Prague. Grzybowski Foundation Special Publication 8:471–483.

Zuo, S. H., N. C. Zhang, B. Li, Z. Zhang, Z. X. Zhu. 2009. Numerical simulation of tidal current and erosion and sedimentation in the Yangshan deep-water harbor of Shanghai. International Journal of Sediment Research 24:287–298.